Rare Metal Materials and Engineering
Volume 53, Issue 1, January 2024
Available online at www.rmme.ac.cn

Science Press

Cite this article as: Nabahat Mehran, Duan Yajuan, Xu Zongrui, et al. Creep and Recovery Behavior of Metallic Glasses: A Short Review[J]. Rare Metal Materials and Engineering, 2024, 53(01): 47-55. DOI: 10.12442/j.issn.1002-185X.E20230837.

REVIEW

Creep and Recovery Behavior of Metallic Glasses: A Short Review

Nabahat Mehran[1], Duan Yajuan[1,2], Xu Zongrui[1,2], Qiao Jichao[2], Pineda Eloi[1]

[1] Department of Physics, Institute of Energy Technologies, Universitat Politècnica de Catalunya-BarcelonaTech, Barcelona 08019, Spain; [2] School of Mechanics, Civil Engineering and Architecture, Northwestern Polytechnical University, Xi'an 710072, China

Abstract: Due to the disordered structure of amorphous alloys, the complex structural dynamics involves the particle rearrangements with a large span in time and size scales. The characterization and mechanism of structural dynamics of amorphous alloys are crucial and fundamental for the further research of relaxation behavior and physical aging kinetics of glasses. Abundant researches show that the relaxation spectra of rare-earth-based amorphous alloys, which are represented by lanthanum- and cerium-based alloys, show obvious secondary relaxation process, and the system becomes an ideal carrier to investigate the relationship between structural dynamics and mechanical properties of amorphous alloys. In this review, the anelasticity of metallic glasses was discussed. The anelastic deformation, as the main component of deformation, can totally recovery after unloading in creep experiments, and its mechanism is important to form deep understanding about the structural dynamics of metallic glasses. Additionally, the main characteristics of anelastic deformation during creep and creep recovery were summarized, and some theoretical models for quantitative and qualitative description were introduced.

Key words: creep; metallic glass; structural dynamics; physical aging kinetics

One of the distinctive properties of disordered matter is the presence of a broad mechanical relaxation spectrum covering several decades of timescales. Metallic glasses, or amorphous alloys, are particular disordered materials, whose constituent particles comprise various types of atoms (two or more species) with characteristics of low direction, metallic-like identity, and interatomic bonds. By fast quenching from the liquid, crystallization can be avoided, glass transition can be achieved, and the metallic glass forms. Through deposition technique, more stable metallic glass can be approached[1]. Some metallic glass-forming systems develop based on the rare-earth elements, particularly the cerium- and lanthanum-series elements, as well as praseodymium, neodymium, samarium, dysprosium, and erbium[2]. Ce- and La-based metallic glasses have outstanding glass-forming ability, and their glass transition temperature is between 100 and 250 °C. Some metallic glasses even present the polyamorphic (liquid-liquid or glass-glass) transitions[3].

The particle dynamics of disordered systems has different processes. In the short timescale, the vibrational dynamics of amorphous systems attracts much attention. The Boson peak and the low temperature heat capacity have been widely researched[4–7]. In the long timescale, glasses and amorphous materials show structural dynamics, involving different types of particle rearrangements[8]. Due to thermal activation, the molecules can rearrange their positions and explore new local configurations in the continuous collective "microscopic dance". This process is very fast for the materials with low packing densities at high temperatures but extremely slow for the ones with well relaxed glass structures at low temperatures. When an external force is applied onto the material, the molecule positions are rearranged to relax and adapt to the new external conditions, which is attributed to the structural dynamics.

To investigate the relaxation dynamics, strain or stress is

Received date: December 26, 2023
Foundation item: Investigación Financiado por MCIN/AEI/10.13039/501100011033 (Proyecto PID2020-112975GB-I00); Generalitat de Catalunya AGAUR (2017-SGR-42); Innovation Foundation for Doctor Dissertation of Northwestern Polytechnical University (CX202031); supported by China Scholarship Council (202006290092, 202206290063); National Natural Science Foundation of China (51971178, 52271153); Natural Science Basic Research Plan for Distinguished Young Scholars in Shaanxi Province (2021JC12)
Corresponding author: Pineda Eloi, Ph. D., Professor, Department of Physics, Institute of Energy Technologies, Universitat Politècnica de Catalunya-BarcelonaTech, Barcelona 08019, Spain, Tel: 0034-935-521141, E-mail: eloi.pineda@upc.edu

Copyright © 2024, Northwest Institute for Nonferrous Metal Research. Published by Science Press. All rights reserved.

usually applied. After applying a constant strain, the stress relaxation can be monitored[9]. After applying a constant stress, the strain is measured, namely the creep experiment. Creep is an important behavior for glasses at high energy configurational states or at the temperatures approaching the glass transition.

This review summarized the basic features of anelastic response in creep experiments, presenting comprehensive results of the deformation of metallic glasses as much as possible.

1 Creep Behavior of Metallic Glasses

1.1 Viscoelasticity

In the creep experiment, a constant load is applied to the material, the resultant strain response exhibits various components, and each component can be distinguished by its temporal behavior, recoverability upon stress removal, and linear or non-linear nature. Within the linear response, primary strain components can be distinguished, as follows.

(1) Elasticity: this component represents instantaneous deformation upon stress and instantaneous recoverability after stress release. With small strains, this component is usually linear and obeys the Hook's law $\varepsilon=\sigma/E$, where ε is the strain, σ is the stress, and E is the elastic modulus. For the amorphous materials, it is worth noting that the elasticity may be caused by both affine and non-affine atomic displacements[10-11], leading to lower elastic modulus, compared with that of the crystalline counterpart. In many amorphous polymers, the elastic component shows the non-Hookean stress-strain dependence, which is related to the entropic elasticity effects. However, the non-Hookean elasticity cannot be observed in amorphous metals.

(2) Anelasticity: the anelastic behavior can be defined as the delayed elasticity, which contributes to the deformation and is totally recoverable after the release of external stress. Anelasticity implies the existence of particle rearrangements in the material. Amorphous materials have various anelastic modes, covering many decades of timescales[12]. The distribution of anelastic modes and its relationship with the structural rearrangement in metallic glasses requires further investigation[13].

(3) Viscous plasticity: this component leads to permanent deformation. During the Newtonian behavior, the viscous plasticity obeys the linear stress-strain relationship $\mathrm{d}\varepsilon/\mathrm{d}t = \sigma/\eta$, where η is the viscosity and the amount of permanent deformation; t is the time. Viscous flow is proportional to time and stress. The viscosity of amorphous materials mainly depends on the stress. A classical non-linear behavior is modeled by the Eyring dashpot, where the activation energy for viscous flow is reduced by stress[14]. The Eyring dashpot can model the steady state flow of metallic glasses[15–17].

The Hookean elastic response is associated with the ideal solid, whereas the Newtonian viscous response is associated with the ideal liquid. Metallic glasses and glass-forming supercooled liquids behave as viscoelastic materials in the linear regime, which are transformed from solid to liquid, depending on the ratio of the inner relaxation time of material to the characteristic timescale of external mechanical stimulus.

In addition to the abovementioned three factors, other stress-strain behavior can also be observed. Instantaneous plasticity, namely instantaneous permanent deformation or strain jump, can be found in many materials during mechanical experiments. This behavior is the consequence of inhomogeneous concentration of strain in a localized zone of material, i.e., the creation and slip of shear bands in metallic glasses. The linearity between stress and strain always disappears after the stress/strain exceeds a certain critical value. In addition to intermittent plastic events and non-homogeneous flow at low temperatures, the non-Newtonian viscosity with strain-rate-dependence and non-linearity relationship of stress with strain can be observed in the metallic glass-formers under high stresses or high strain rates. Furthermore, the stress-strain behavior can also be modified by geometrical constrains, such as necking, barreling, or size effects[18].

1.2 Creep compliance in linear response regime

If the creep experiment is conducted at low stress (linear regime) and the strains are small enough to neglect the geometrical effects, such as necking, the creep behavior of metallic glasses can be described by three primary linear components, as follows:

$$\frac{\varepsilon(t)}{\sigma} = J(t) = M^{-1} + J_{\mathrm{a}}\phi_{\mathrm{r}}(t) + \frac{t}{\eta} \tag{1}$$

where $J(t)$ is the creep compliance, M is the elastic modulus, J_{a} is the intensity of recoverable anelastic strain, $\phi_{\mathrm{r}}(t)$ is the creep retardation function, and η is the viscosity (extensional viscosity for tensile experiments). The retardation function changes from $\phi_{\mathrm{r}} = 0$ at $t = 0$ to $\phi_{\mathrm{r}} = 1$ at $t \to \infty$, and it can be regarded as the response of distribution $D_{\mathrm{r}}(\tau)$ of anelastic deformation modes, as follows:

$$\phi_{\mathrm{r}}(t) = \int_0^{\infty} D_{\mathrm{r}}(\tau)\left[1 - \mathrm{e}^{-\frac{t}{\tau}}\right]\mathrm{d}\tau \tag{2}$$

Fig. 1 shows the creep experiment results of annealed $Pd_{82}Si_{18}$ metallic glass[19]. The pre-annealing treatment was performed at 500 K for 343 h, which can ensure the iso-configurational state during the creep experiments. Three basic strain components can be clearly observed. The ratio of the anelastic deformation to the elastic deformation of metallic glasses, $\varepsilon_{\mathrm{anelastic}}/\varepsilon_{\mathrm{elastic}} = J_{\mathrm{a}}M$, is changed with varying the temperature. This ratio is small at low temperatures, but it is around 1 at the temperatures not far below the glass transition temperature[20]. Fig. 2 shows the disappearance of linearity when the stress is above 300 MPa for the $Pd_{82}Si_{18}$ metallic glass[21]. Fig. 3 shows the linear behavior of both viscosity and plastic strain of Vit4 metallic glass[20]. The linear response can be observed at different temperatures when the stress is below 250 MPa. The nonlinear behavior appears when the stress is around 400 MPa at 580 K.

All strain components, $\varepsilon_{\mathrm{elastic}}$, $\varepsilon_{\mathrm{anelastic}}$, and $\varepsilon_{\mathrm{plastic}}$, show linear relationship with the stress in the relaxed material. To reach the relaxed state, the material is annealed at the same temperature for basically the same duration as those of creep experiments. Therefore, for the as-annealed samples, their structural state can be considered as the unchanged state, or it

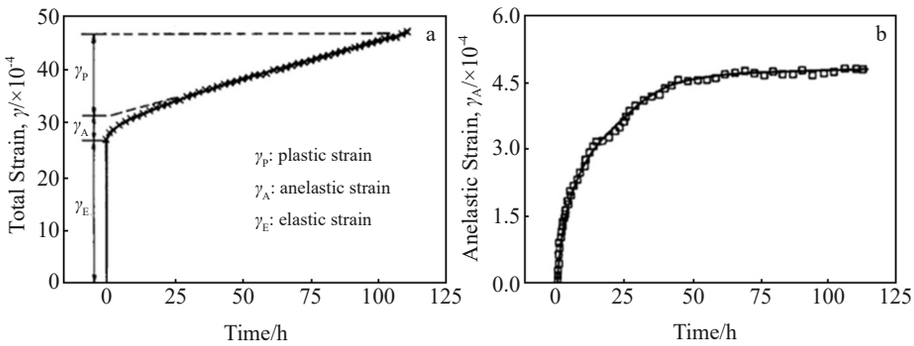

Fig.1 Creep experiment results of as-annealed $Pd_{82}Si_{18}$ metallic glass wires at 500 K[19]: (a) total strain and (b) anelastic strain

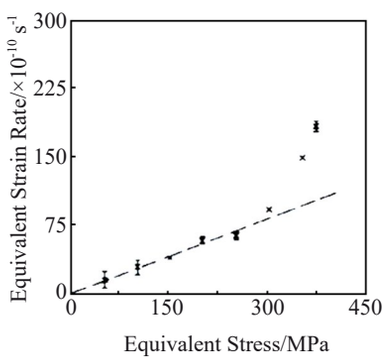

Fig.2 Relationship between equivalent strain rate and equivalent stress of $Pd_{82}Si_{18}$ metallic glass wires[21]

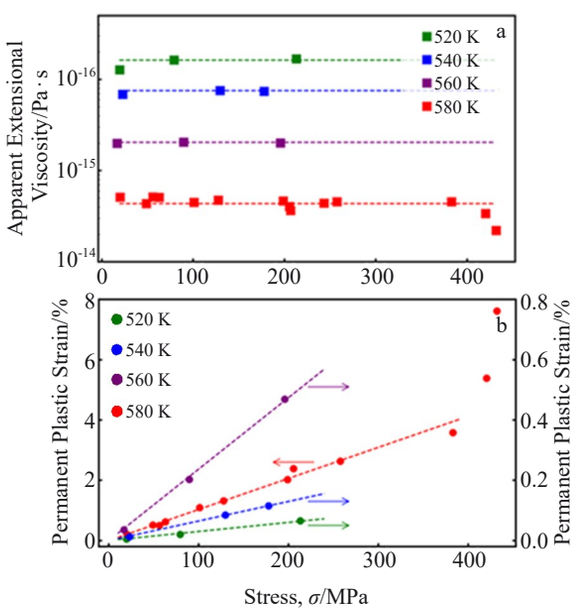

Fig.3 Apparent extensional viscosity (a) and permanent plastic strain (b) of Vit4 metallic glass after creep for 600 min[20]

evolves really slow in the experimental timescale. The viscoelastic behavior of metallic glasses is in agreement with the ideal behavior, presenting clear separation of elastic, anelastic, and plastic contributions. However, the non-equilibrium nature of glasses causes the easy variation of structure by physical rejuvenation and aging during thermal and mechanical treatments, resulting in more difficulties in the interpretation of experiment phenomena.

1.3 Creep behavior of iso-configurational metallic glasses

The anelastic modes of metallic glasses are thermally activated[22]. The reversible component of creep flow is controlled by the distribution of activation energy $D(E)$, which can be transformed into the distribution of relaxation time $\ln\tau = \ln\tau_0 + E/kT$ with $\tau_0=10^{-12}-10^{-14}$ s and k as the Boltzmann constant. Due to the anharmonicity and thermal expansion, some small changes are neglected, and the distribution of energy barriers can be regarded as a specific property of particular glass configuration when the structural aging or rejuvenation is not conducted. Fig.4 shows the creep behavior calculated by Eq. (1) and Eq. (2) under the assumption that the distribution of activation energies does not change with time. Fig.4a shows the distribution of activation energies; Fig.4b shows the corresponding distribution of lgτ during creep experiment at temperature T=580 K; Fig. 4c shows the calculated creep rates from 1 s to 3×10^4 s.

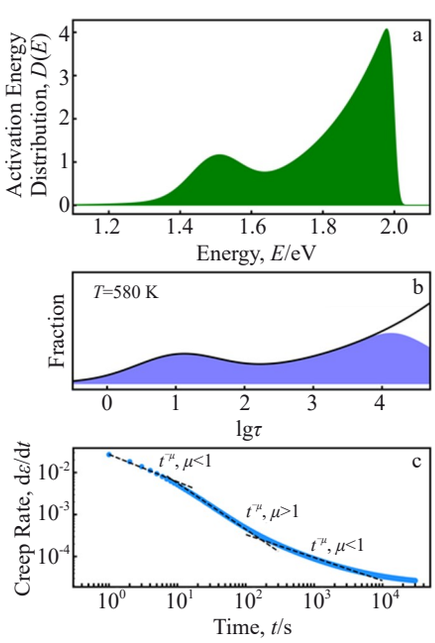

Fig.4 Activation energy distribution $D(E)$ of anelastic mode of simulation model (a); distribution of lgτ calculated from $D(E)$ during creep experiment at temperature T=580 K (b); calculated creep rates from 1 s to 3×10^4 s (c)

The derivative in time of the anelastic component of Eq.(1) is mathematically equivalent to the Laplace transform result of the distribution of anelastic mode frequencies. Therefore, with the flat distribution of activation energies and a constant viscosity, the creep rate can be calculated, as follows:

$$\frac{\mathrm{d}\varepsilon(t)}{\mathrm{d}t} = At^{-\mu} + \frac{\sigma}{\eta} \tag{3}$$

where μ is local exponent with μ=1. This relationship can be used to predict the distribution shape of activation energies with creep rate. When the anelastic modes have the distribution with positive slopes ($\mathrm{d}D(E)/\mathrm{d}E>0$), $\mu<1$; otherwise, $\mu>1$, as shown in Fig.4c.

Then, by estimating the local exponent μ in a certain region of time, the occurrence of peaks in the distribution of relaxation time can be easily detected from the creep rate. In the long timescale, in addition to the longest relaxation mode with the anelastic distribution, the creep rate tends to be constant as $\sigma\eta^{-1}$, and it is eventually controlled by the steady state viscosity.

1.4 Creep and recovery of rejuvenated/aged metallic glasses

The characteristic of glass state involves the out-of-equilibrium nature. Crystalline and liquid phases are in thermodynamic stable state or present metastable configurations at fixed pressure and temperature conditions. Even when the supercooled liquids are at metastable state, their configurations correspond to the well-defined minimum free energy, i.e., under the fixed external pressure (P) and temperature (T), any state property f of the metastable phase (density, enthalpy, entropy) has unique value $f(P, T)$. The properties of the out-of-equilibrium glass depend on the previous pressure-temperature-time path, and the glass state has memory. The glass configuration can be quantified by the fictive temperature T_f[23] and the glass properties depend on the parameter $f = f(P, T, T_f)$. As shown in Fig. 5, the ideal metastable supercooled liquid corresponds to $T_f \rightarrow T$, which indicates the most stable glass configuration at temperature T. Physical aging and rejuvenation correspond to the decrease and increase in T_f, respectively.

Excess free volume v_f can be used to interpret the structural changes during aging and rejuvenation of metallic glasses[24-25]. The structural states of high fictive energy (rejuvenated states) are associated with the configurations with large excess free volume in the structure, whereas the stable states of low fictive temperature (aged states) correspond to small v_f. Based on the free volume concept, the steady state homogeneous flow of metallic glasses at high temperatures can be modeled[16–17], considering that the material reaches the balance of free volume due to the compensation between deformation and annihilation during annealing. Similar results can be obtained through other physical concepts to quantify the structural glass state, such as the concentration of point defects[26].

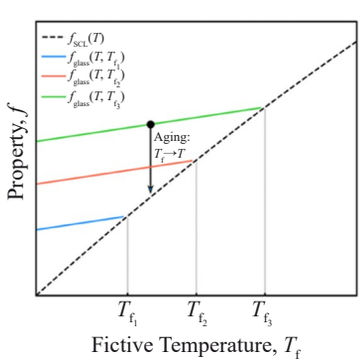

Fig.5 Schematic diagram of property variation as function of temperature under constant pressure for supercooled liquid (dashed line) and materials with different glass states and fictive temperatures

Simultaneous change of structure causes difficulty in investigation of creep behavior of metallic glasses, because annealing (aging) and deformation (rejuvenation) may occur during creep experiment. The viscoelasticity of glasses is dependent on the structural state of glasses (fictive temperature), implying that it can be constantly changed through aging or rejuvenation during thermo-mechanical experiments. The three terms in Eq. (1) are all dependent on the fictive temperature. With decreasing the T_f value (with increasing the glass density and stability), both the elastic modulus $M(T, T_f)$ and the viscosity $\eta(T, T_f)$ are increased, whereas the anelastic mode distribution $D_r(T, T_f, \tau)$ is shifted towards the long time region. Therefore, even during the ideal creep tests with small strains, the elastic, anelastic, and viscous components of the glass may have time dependence through $T_f(t)$.

Fig.6 shows the difference between two consecutive cycles of creep and recovery of $Pd_{80}Si_{20}$ glass[27]. The elastic creep (ε_0), transient creep (ε_1), viscous creep (ε_2) components, as well as the corresponding elastic recovery (ε_3), anelastic recovery (ε_4), and plastic recovery (ε_5) components are presented in Fig.6, and their values are listed in Table 1. The first cycle is affected by structural changes during creep test, resulting in a large difference between the transient creep amplitude (ε_1) and anelastic recovery (ε_4). However, in the second cycle, $\varepsilon_1 \approx \varepsilon_4$. Besides, the amount of irreversible deformation (ε_5) can be attributed only to the pure viscous contribution (ε_2), thus $\varepsilon_2 \approx \varepsilon_5$.

Therefore, Eq. (1) with constant M, η, and $D_r(\tau)$ can appropriately describe the creep behavior of well annealed iso-

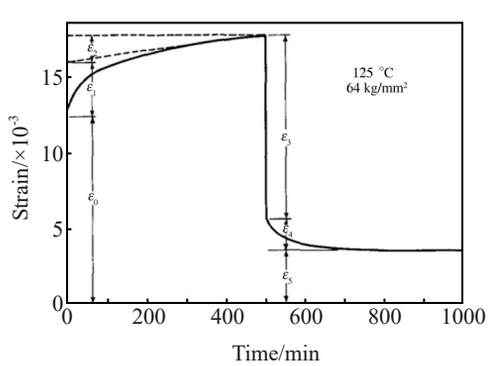

Fig.6 Creep and creep recovery curves of $Pd_{80}Si_{20}$ glass[27]

Table 1 Creep and recovery parameters of $Pd_{80}Si_{20}$ glass under conditions of 150 °C, 53 kg/mm², and 800 min (×10⁻³)[27]

Cycle No.	ε_0	ε_1	ε_2	ε_3	ε_4	ε_5	$\varepsilon_1-\varepsilon_4$	$\varepsilon_1+\varepsilon_2$
1	9.99	5.07	2.50	9.76	2.21	5.59	2.86	7.57
2	9.71	1.92	2.10	9.62	1.90	2.21	0.02	4.02

configurational metallic glass in the linear stress deformation region. However, these conditions cannot always be fulfilled in most creep studies: the region of stress and deformation may be above the linear region, where the glass structure changes during the test because of aging, annealing, rejuvenation, mechanical deformation, or combined effects.

2 Creep Behavior Models of Metallic Glasses

2.1 Empirical functions

By adjusting the experiment curves, a common analysis can be conducted to characterize the creep behavior:

$$\varepsilon(t)-\varepsilon_{\text{elastic}}=\sum_{i=1}^{n}\varepsilon_i\left(1-\mathrm{e}^{-t/\tau_i}\right)+\sigma t/\eta_0 \quad (4)$$

where ε_i and τ_i are the intensity and time of the ith anelastic mode, respectively.

The total number of modes n is used to adjust the experiment data. In most cases, one mode per decade can accurately reproduce the creep curves. For instance, the creep of Mg-Cu-Y metallic glasses was studied by nanoindentation, and the time dependence of indentation depth under constant load was modeled by Eq.(4) with n=2[28]. In Ref.[28], the temporal resolution has the order of 1 s and the total duration of the nanoindentation creep tests is around 100 s. Considering two modes with 1 s<τ_1<10 s and 10 s<τ_2<100 s, the creep curves can be obtained, as shown in Fig. 7. The creep and recovery nanoindentation curves are fitted by anelastic components with different modes and $\varepsilon(t)_{\text{anelastic}}=\varepsilon_1\left(1-\mathrm{e}^{-t/\tau_1}\right)+\varepsilon_2\left(1-\mathrm{e}^{-t/\tau_2}\right)$.

Due to the broadness of exponential relaxation, continuous distribution of modes can be well approached, considering 2–3 modes per decade. The total number of modes for creep curve modeling is then related to the time scale, involving the time resolution and the experiment duration. It is worth noting that too many discrete modes per decade in Eq.(4) can lead to calculation by fitting algorithm. A multimodal distribution of anelastic time with more than two peaks per decade is totally equivalent to a continuous distribution of experimental creep curve. Fig. 8 shows related schematic diagrams. The creep curves corresponding to flat (blue) or multimodal (red) distribution, which contain the same average number of relaxation modes per decade, can hardly be distinguished.

Another common method to characterize creep performance is to fit the experiment curve with the stretched exponential, as follows:

$$\varepsilon(t)-\varepsilon_{\text{elastic}}=\varepsilon_{\text{anelastic}}\left[1-\mathrm{e}^{-\left(t/\tau_{\text{kww}}\right)^{\beta_{\text{kww}}}}\right]+\sigma t/\eta_0 \quad (5)$$

where the parameters τ_{kww} and β_{kww} are characteristic time and stretching exponent, respectively. The exponent β_{kww}<1 quantifies the broadness of retardation time distribution: the smaller the exponent, the broader the distribution of anelastic modes. Generally, Eq. (5) is a good representation of the experiment data when the anelastic mode distribution does not contain peaks, which are supposed to separate in time scale[20].

However, two relaxation processes can be commonly observed in metallic glasses[29–30], especially in the rare-earth (La and Ce) and Pd-based alloys. In many La-based alloys, a distinct β relaxation process is well separated in timescale from the main α relaxation and the creep compliance can be well modeled by Eq.(6), as follows:

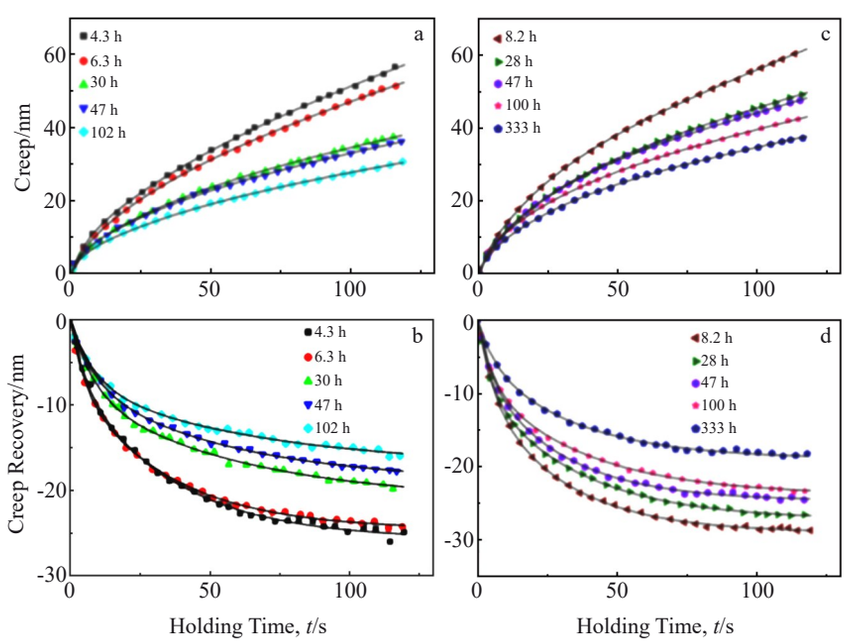

Fig.7 Creep (a, c) and recovery (b, d) nanoindentation curves of $Mg_{65}Cu_{25}Y_{10}$ metallic glass (a–b) and $Mg_{85}Cu_5Y_{10}$ metallic glass (c–d)[28]

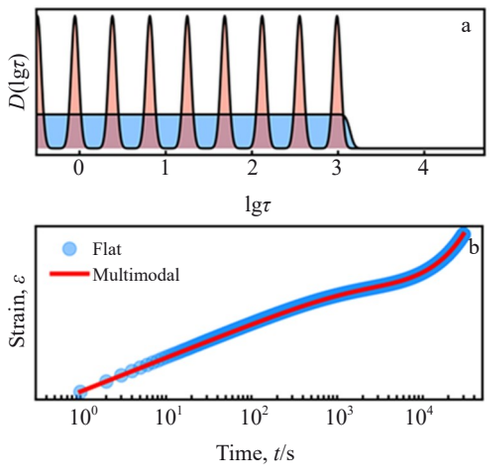

Fig.8 Flat and multimodal distributions of retardation time (a); creep deformation calculated by Eq. (1) and Eq. (2) corresponding to flat and multimodal distributions (b)

$$J(t) = J_{\text{elastic}} + J_{\text{anel},\beta}(t) + J_{\text{anel},\alpha}(t) + J_{\text{viscous}}(t) = M^{-1} + A_{\beta}\left[1 - \mathrm{e}^{-\left(t/\tau_{\beta}\right)^{\gamma_{\beta}}}\right] + A_{\text{an},\alpha}\left[1 - \mathrm{e}^{-\left(t/\tau_{\text{an},\alpha}\right)^{\gamma_{\text{an},\alpha}}}\right] + t/\eta_0 \quad (6)$$

Eq. (6) implies the following facts[13]: the deformation associated with the β relaxation mode A_{β} and most part of the high frequency tail of α relaxation $A_{\text{an},\alpha}$ is reversible and contributes to the anelastic component, whereas the viscous permanent deformation is related to the longest timescale of the α relaxation which determines the material viscosity. The analysis of stress relaxation in step strain experiments confirms this reversible nature of the whole high frequency (or low temperature) wing of the dynamic spectrum of metallic glasses[31], as shown in Fig. 9. As shown in Fig. 9c, the stress relaxation curves at different temperatures have characteristic double decay, and the timescale of the two processes is several orders of magnitude apart below the glass transition temperature.

There are more functional shapes to describe experimental creep curves based on different types of viscoelastic models or empirical functions. However, for the metallic glasses, simple functional shapes mentioned in this research are commonly used to quantify and characterize the anelastic and viscous components of creep. Eq.(5) or Eq.(6) presents less details of the shape of retardation time distribution, compared with Eq. (4), but it presents a more robust analysis to reduce the number of fitting parameters and the risk of mathematical calculation.

2.2 Microscopic models of creep and recovery

The first microscopic picture of creep and recovery in metallic glasses is reported in Ref.[22]. The material contains shearable zones, which is later termed as shear transformation zones (STZs) and visualized as particular types of local atomic arrangements to be shear-transformed by thermal activation. To be shear-transformed, different types of local configurations have to surmount different energy barriers. These local shear-transformation centers are continuously activated along random directions in the stress-free material. But after the application of an external load, the local shear-transformation centers are biased or polarized towards the direction of external stress (Fig. 10). After releasing the external load, they become progressively "de-polarized", because the thermally activated shear transformations become unbiased and randomly oriented again. These structural "polarization" and "de-polarization" processes account for the anelastic recoverable deformation, and the distribution of energy barriers $D(E)$ of the shear-transformation centers defines the distribution of anelastic modes $D_{\tau}(\tau)$ at a given temperature. The viscous permanent deformation is visualized as contiguous deformation with no memory of the initial state.

The microscopic model can explain many basic features of creep behavior of metallic glasses, such as the ability to induce structural anisotropy by applying stress during annealing[32–33]. For instance, the anelastic modes with characteristic time of τ=10^2 s at 500 K (E =1.49 eV) become the ones with τ =10^3 s at 469 K and τ=10^{12} s at 300 K. Thus, the anelastic "polarization" is introduced during deformation at 500 K for 100 s, and it causes the permanent structural change once the material is quenched at room temperature. Au-, Ca-, Ce-, and Mg-based metallic glasses show glass transition temperatures

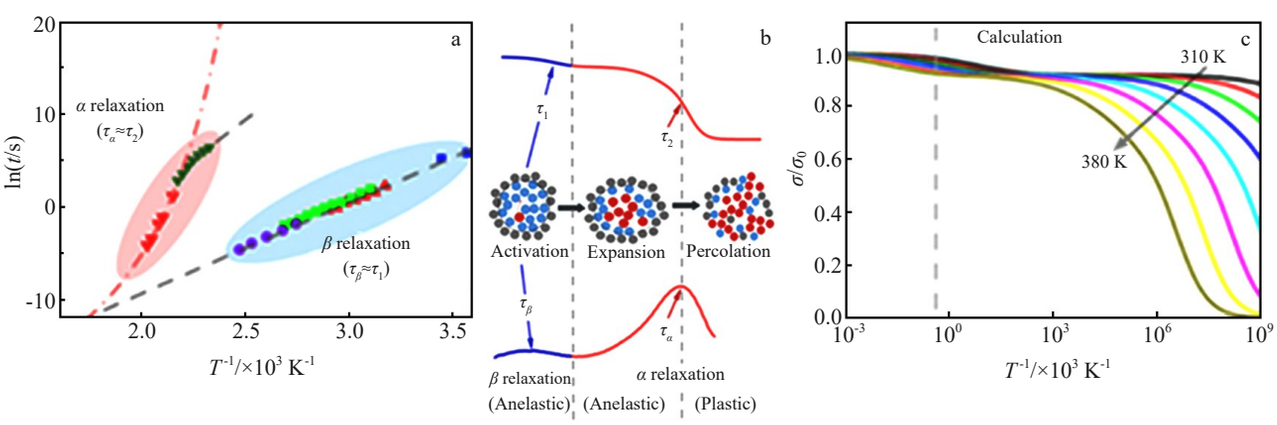

Fig.9 Temperature behavior of relaxation time of α and β relaxation processes in $La_{60}Ni_{15}Al_{25}$ metallic glass (a); storage and loss relaxation modulus corresponding to reversible anelastic relaxation (b); stress relaxation curves at different temperatures (c)[31]

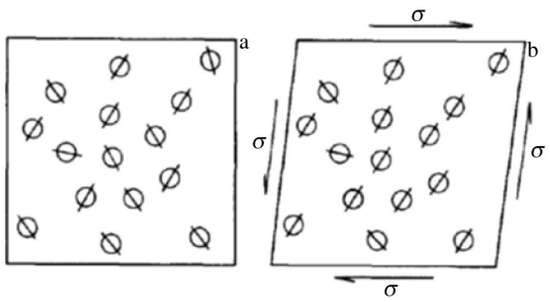

Fig.10 Local shear transformations in external stress-free material (a) and in shear-transformed material (b) leading to inelastic strain[22]

at 325–450 K; La-, Pr-, Pt-, and Pd-based metallic glasses show glass transition temperatures at 450–600 K; Zr-, Hf-, and Cu-based metallic glasses show glass transition temperatures at 600–750 K; Fe- and Ni-based metallic glasses show glass transition temperatures above 750 K. These parameters promote the recoverable structural changes at high temperatures. But the structural changes become permanent during the whole service life at the temperatures below the working temperatures by tens or hundreds of degrees. Rejuvenation strategies are designed based on this memory effect[34].

The microscopic model has been modified in different ways to describe the creep behavior. Perez et al[35] proposed that the anelastic deformation is conducted by the formation of shear microdomains (SMDs). The density of such SMDs in the material depends on the concentration of point defects in the amorphous structure or the order parameter χ form 0 (fully ordered) to 1 (fully disordered). The order parameter contains the information of amorphous state, which is similar to the free volume or the fictive temperature parameters, thus promoting the modeling of deformation behavior with aging or rejuvenation occurrence. Ulfert et al[36] proposed a comprehensive model for both anelastic and viscous deformation. In this model, local "shearable" atoms with given characteristic anelastic time τ nucleate and dissolve. The material is deformed under the external load, producing the macroscopic anelastic deformation, and it is relaxed after unloading. However, the material has a "life time" after the local arrangement becomes permanent. In this case, the material cannot be relaxed, thus producing the irreversible viscous component. Under the stationary conditions, the nucleation of reversible shear centers and their annihilation after the service time lead to the stationary distribution $D_r(\tau)$. With the application of the creep behavior model of Zr-based metallic glass, which does not have evident β relaxation, it is found that the distribution of anelastic modes obeys $D_r(\tau) \propto \tau^{-n}$ relationship with $n \approx 0.6$. This result is in agreement with the relaxation modes with high frequency wing of the α relaxation[20].

Further investigation of the local units related to the anelastic deformation has been widely conducted[37–39]. In Al- and La-based metallic glasses, the distribution of anelastic units with retardation and recovery times τ_i can be identified by STZs of different sizes. The model involves STZs with characteristic volumes Ω_i and $\Omega_{i+1} = \Omega_i + \Delta\Omega$, where $\Delta\Omega$ is related to the order of one atomic volume. The fast anelastic modes correspond to the β relaxation, whereas the long ones correspond to the α relaxation.

Molecular dynamics simulations have also been used to investigate the creep mechanisms. It is worth noting that the experiment timescale and iso-configurational state in simulation are quite different from those in real materials. Extremely long simulations may reach the timescale order of microseconds, whereas the duration of creep experiments is usually $1–10^5$ s. Cao et al[40] found that above a certain level of applied load, the creep deformation in the simulated $Cu_{50}Zr_{50}$ metallic glass is driven by the activation of shear transformations in localized zones, as shown in Fig. 11, whereas the homogeneous diffusional-like mechanism dominates the creep at low stresses. Therefore, the simulations confirm the existence of microscopic mechanisms, which are similar to the local shear transformations in the creep models. However, the anelastic performance and recovery behavior, the characteristic of metallic glasses, still require deep investigation. As shown in Fig.9, in the iso-configurational glass, almost all structural processes with duration shorter than the timescale of α relaxation peak correspond to the reversible deformation modes.

Hierarchical views of the anelastic modes have been recently extended[13]. Inspired by the model of constrained motion of structural units in metallic glasses[41] and the concentration of point defect model[35], the models of STZs (or SMDs) nucleation, expansion, and vanishing have been proposed. The expansion of the deformation centers generates the retardation time distribution, because the small deformation centers deform faster than the big ones do when they are activated under external stress. After a certain service time, the deformation centers vanish, generating permanent viscous deformation. The service time of SMDs is associated with the percolation of the expansion of deformation centers, considering that the reverse driving force from the surrounding elastic matrix is cancelled when the growing SMDs overlap with each other. The model can produce the creep and stress relaxation features of La-based metallic glasses, which shows prominent β relaxation.

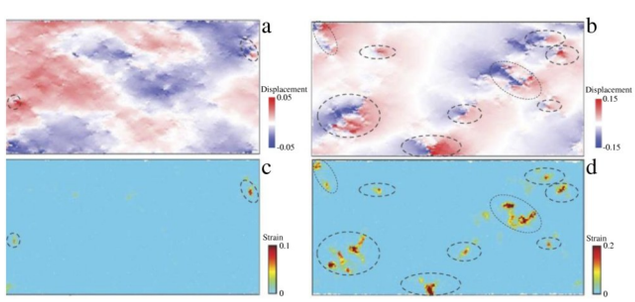

Fig.11 Spatial maps of non-affine displacement (a–b) and deviatoric strain (c–d) in simulated $Cu_{50}Zr_{50}$ metallic glass under creep with low external stress (a, c) and high external stress (b, d)[40]

Different microscopic views have also been proposed[42]. The creep curve is analyzed based on the waiting time for displacement of 15 nm in Pd-based MG. The statistics results of the waiting time show the frequency distribution, obeying different exponential laws for short and long time. The creep behavior depends on the level of applied stress and test temperature (Fig. 12). It is found that the waiting time is related to the avalanche-like process, indicating the formation of nano-shear bands induced by cooperative activation of STZs. During the long creep process, the formation of new nano-shear bands is gradually decreased and the deformation continues by the cooperative motion within the network of preformed nano-shear bands. This microscopic model of nano-avalanches may be related to the expansion of STZs in other models, but the mechanism is still obscure. The reasons for the reversible creep deformation when the external load is released should be further researched.

Finally, the relation between the stress relaxation and creep experiments should be discussed. The origin and behavior of the β relaxation in metallic glasses are important investigation subjects. The increase/decrease in structural heterogeneity during rejuvenation/aging processes can be well characterized by both the change in intensity and shift in timescale of the β relaxation[43–44]. Within the linear region (small strain) under non-aging conditions (well relaxed with slow aging rate), the relaxation and retardation spectra are intrinsically related. The retardation spectra usually shift towards longer timescale. Although the same information about the relaxation dynamics can be obtained from creep and stress relaxation, different experiments are sensitive to different aspects of the relaxation dynamics. The clear β process in the relaxation spectrum of rare-earth-based metallic glasses corresponds to the timescale of seconds or several minutes at the common creep temperatures. Only the initial part of creep process is related to the β relaxation of metallic glasses. Therefore, the important changes of creep behavior due to the evolution of structural heterogeneity provide unique insights on the effects of structural heterogeneity on the long timescale dynamics.

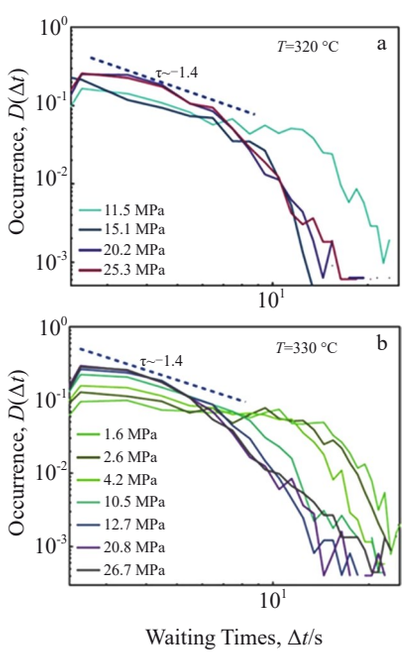

Fig.12 Distribution of waiting time for displacement of 15 nm during creep process of $Pd_{77.5}Cu_6Si_{16.5}$ metallic glass[42]

3 Conclusions

The basic behavior in creep and recovery processes was summarized. Metallic glasses, in the small stress linear regime, behave as ideal viscoelastic materials with wide spectrum of structural dynamic processes and characteristic times covering many decades. Most part of this distribution corresponds to the reversible modes, where the material is relaxed to its original size after the external load is released. The anelastic particle rearrangements are thermally activated, implying that the reversible structural changes can be frozen by quenching after creep experiment, which can modify the isotropic nature of the glass state and explore new configurations of the potential energy landscape.

What is the microscopic nature of these reversible structural rearrangements? Some classic models were reviewed in this research, but the available microscopic models cannot perfectly describe the anelastic recoverable strain of metallic glasses. The shear transformation zones or shear microdomains with energy barrier reduced by stress provide good models for the homogeneous steady-state permanent deformation of metallic glasses.

However, the creep under small stresses is mainly attributed to the recoverable strain, which is directly related to the underlying distribution of structural dynamic processes. In this case, the microscopic description is not established yet. This review presents the basic features of comprehensive models and the mechanisms of the anelastic component of metallic glass deformation, providing guidance for the further research of creep performance of metallic glasses.

References

1 Lüttich M, Giordano V M, Floch S *et al*. *Physical Review Letters*[J], 2018, 120(13): 135504

2 Suryanarayana C, Inoue A. *Bulk Metallic Glasses*[M]. Boca Raton: CRC Press, 2011

3 Shen J, Lu Z, Wang J Q *et al*. *Journal of Physical Chemistry Letters*[J], 2020, 11(16): 6718

4 Vasiliev A, Voloshok T, Granato A *et al*. *Physical Review B*[J], 2009, 80(17): 172102

5 Derlet P M, Maaß R, Löffler J F. *The European Physical Journal B*[J], 2012, 85(5): 148

6 Mitrofanov Y P, Peterlechner M, Divinski S V *et al*. *Physical Review Letters*[J], 2014, 112(13): 135901

7 Crespo D, Bruna P, Valles A *et al*. *Physical Review B*[J], 2016, 94(14): 144205

8 Angell C A, Ngai K L, McKenna G B *et al*. *Journal of Applied Physics*[J], 2000, 88(6): 3113

9 McKenna G B. *Journal of Physics: Condensed Matter*[J], 2003,

15(11): S737
10 Knuyt G, Schepper L D, Stals L M. *Journal of Physics F: Metal Physics*[J], 1986, 16(12): 1989
11 Pineda E. *Physical Review B*[J], 2006, 73(10): 104109
12 Argon A S. *Journal of Applied Physics*[J], 1968, 39(9): 4080
13 Hao Q, Lyu G J, Pineda E *et al*. *International Journal of Plasticity*[J], 2022, 154: 103 288
14 Bauwens-Crowet C, Bauwens J C. *Journal of Materials Science*[J], 1975, 10(10): 1779
15 Spaepen F. *Acta Metallurgica*[J], 1977, 25(4): 407
16 Bletry M, Guyot P, Blandin J J *et al*. *Acta Materialia*[J], 2006, 54(5): 1257
17 Bletry M, Guyot P, Bréchet Y *et al*. *Acta Materialia*[J], 2007, 55(18): 6331
18 Kumar G, Desai A, Schroers J. *Advanced Materials*[J], 2011, 23(4): 461
19 Taub A I, Spaepen F. *Journal of Materials Science*[J], 1981, 16(11): 3087
20 Nabahat M, Amini N, Pineda E *et al*. *Physical Review Materials*[J], 2022, 6(12): 125601
21 Taub A I. *Acta Metallurgica*[J], 1980, 28(5): 633
22 Argon A S, Kuo H Y. *Journal of Non-crystalline Solids*[J], 1980, 37(2): 241
23 Moynihan C T, Easteal A J, Bolt M A *et al*. *Journal of the American Ceramic Society*[J], 1976, 59(1–2): 12
24 Cohen M H, Turnbull D. *The Journal of Chemical Physics*[J], 1959, 31(5): 1164
25 Turnbull D, Cohen M H. *The Journal of Chemical Physics*[J], 1970, 52(6): 3038
26 Cheng Y T, Hao Q, Pelletier J M *et al*. *International Journal of Plasticity*[J], 2021, 146: 103107
27 Maddin R, Masumoto T. *Materials Science and Engineering*[J], 1972, 9(C): 153
28 Castellero A, Moser B, Uhlenhaut D I *et al*. *Acta Materialia*[J], 2008, 56(15): 3777
29 Ruta B, Chushkin Y, Monaco G *et al*. *Physical Review Letters*[J], 2012, 109(16): 165701
30 Duan Y J, Zhang L T, Qiao J C *et al*. *Physical Review Letters*[J], 2022, 129(17): 175501
31 Hao Q, Pineda E, Wang Y J *et al*. *Physical Review B*[J], 2023, 108(2): 24101
32 Sun Y H, Concustell A, Carpenter M A *et al*. *Acta Materialia*[J], 2016, 112: 132
33 Kozikowski P, Ohnuma M, Hashimoto R *et al*. *Physical Review Materials*[J], 2020, 4(9): 95 604
34 Ketov S V, Sun Y H, Nachum S *et al*. *Nature*[J], 2015, 524(7564): 200
35 Perez J. *Acta Metallurgica*[J], 1984, 32(12): 2163
36 Ulfert W, Kronmüller H. *Le Journal de Physique IV*[J], 1996, 6(C8): C8-617-C8-620
37 Ju J D, Jang D, Nwankpa A *et al*. *Journal of Applied Physics*[J], 2011, 109(5): 53522
38 Ju J D, Atzmon M. *Acta Materialia*[J], 2014, 74: 183
39 Lei T J, Da Costa L R, Liu M *et al*. *Physical Review E*[J], 2019, 100(3): 33001
40 Cao P, Short M P, Yip S. *Proceedings of the National Academy of Sciences*, 2017, 114(52): 13631
41 Palmer R G, Stein D L, Abrahams E *et al*. *Physical Review Letters*[J], 1984, 53(10): 958
42 Krisponeit J O, Pitikaris S, Avila K E *et al*. *Nature Communications*[J], 2014, 5(1): 3616
43 Qiao J C, Wang Q, Pelletier J M *et al*. *Progress in Materials Science*[J], 2019, 104: 250
44 Liang S Y, Zhang L T, Wang B *et al*. *Intermetallics*[J], 2024, 164: 108115

金属玻璃蠕变及回复行为研究综述

Nabahat Mehran[1]，段亚娟[1,2]，徐宗睿[1,2]，乔吉超[2]，Pineda Eloi[1]
(1. 加泰罗尼亚理工大学 能源技术研究所 物理系，西班牙 巴塞罗那 08019)
(2. 西北工业大学 力学与土木建筑学院，陕西 西安 710072)

摘　要：由于非晶合金独特的无序结构，其结构动力学特征涉及较大时间与尺寸跨度的粒子重排。作为深入研究金属玻璃体系弛豫行为与老化动力学的基础，对非晶合金结构动力学的表征和理解至关重要。大量研究表明，以镧基和铈基为代表的稀土基非晶合金的弛豫谱呈现明显次级弛豫过程，该体系亦成为探究非晶合金结构动力学与力学性能关联的理想载体。本文主要就金属玻璃的滞弹性变形作了详细评述。作为蠕变实验中变形的主要成分，这类变形在卸载后可完全回复，对其合理描述是深入理解非晶合金结构动力学的关键。此外，总结了蠕变和蠕变回复过程中滞弹性变形的主要特征，并介绍了几种可用于定量或定性分析的理论模型。

关键词：蠕变；金属玻璃；结构动力学；老化动力学

作者简介：Nabahat Mehran，男，1993年生，博士生，加泰罗尼亚理工大学能源技术研究所物理系，西班牙 巴塞罗那 08019，电话：0034-935-521141，E-mail：mehran.nabahat@upc.edu